

**Evidence of the production of hot hydrogen atoms in RF plasmas by catalytic reactions
between hydrogen and oxygen species**

Jonathan Phillips and Chun Ku Chen, Dept. of Chem. And Nucl. Engr., Univ. of New Mexico
and
Randell Mills, BlackLight Power, Cranbury, NJ

Abstract

Selective H-atom line broadening was found to be present throughout the volume (13.5 cm ID x 38 cm length) of RF generated H_2O plasmas in a GEC cell. Notably, at low pressures (ca. <0.08 Torr), a significant fraction (ca. 20%) of the atomic hydrogen was ‘hot’ with energies greater than 40 eV with a pressure dependence, but only a weak power dependence. The degree of broadening was virtually independent of the position studied within the GEC cell, similar to the recent finding for He/H_2 plasmas in the same GEC cell. In contrast to the atomic hydrogen lines, no broadening was observed in oxygen species lines at low pressures. Also, in ‘control’ Xe/H_2 plasmas run in the same cell at similar pressures and adsorbed power, no significant broadening of atomic hydrogen, Xe , or any other lines was observed. Stark broadening or acceleration of charged species due to high electric fields can not explain the results since (i) the electron density was insufficient by orders of magnitude, (ii) the RF field was essentially confined to the cathode fall region in contrast to the broadening that was independent of position, and (iii) only the atomic hydrogen lines were broadened. Rather, all of the data is consistent with a model that claims specific, predicted, species can act catalytically through a resonant energy transfer mechanism to create ‘hot’ hydrogen atoms in plasmas.

I. INTRODUCTION

Plasma sources have been developed over decades as light sources, ionization sources for mass spectroscopy, excitation sources for optical spectroscopy, and sources of ions for surface etching and chemistry. But, only in the last decade has extensive spectroscopic characterization been conducted on “mixed gas” plasmas, and these studies revealed some surprising results for those mixed gas plasmas in which hydrogen was one of the gases. In mixtures of argon and hydrogen, the hydrogen emission lines are significantly broader than any argon line. For example, Kuraica and Konjevic [1-2], Videnovic et al. [3] and others [4-17] have characterized mixed hydrogen-argon plasmas by determining the excited hydrogen atom energies and concentrations from measurements of the line broadening of the 656.3 nm Balmer α line. They found that the H_α lines were extremely broadened and explained the phenomenon primarily in terms of Doppler broadening. They postulated that the energy required to create the ‘hot’ (>20 eV) hydrogen was generated by the acceleration of hydrogen ions such as H^+ , H_2^+ , and H_3^+ in the high fields (e. g. over 10 kV/cm) present in the cathode fall region. Subsequent charge exchange and dissociation of the field accelerated ions left ‘hot’ neutral H atoms.

Djurovic and Roberts [5] recorded the spectral and spatial profiles of Balmer α line emission from low pressure RF (13.56 MHz) discharges in $H_2 + Ar$ mixtures in a direction normal to the electric field. The introduction of Ar in a pure H_2 plasma increased the number of fast neutral atoms as evidenced by the intensity of the broad component of a two-component Doppler-broadened Balmer α line profile. Independent of cell position or direction, the average energy of a wide profile component was 23.8 eV for voltages above 100 V, and the average energy of a slow component was 0.22 eV. The mechanism proposed by Djurovic and Roberts is the production of fast H atoms from electric field accelerated H_2^+ . The explanation of the role of Ar in the production of a large number of excited hydrogen atoms in the $n = 3$ state, as well as raising their energy for a given pressure and applied RF voltage, is that collisions with Ar in the plasma sheath region enhances the production of fast H_2 from accelerated H_2^+ . The fast H_2 then undergoes dissociation to form fast H which may then be excited locally to the $n = 3$ state by a further collision with Ar . The local excitation is a requirement since the atomic lifetime of the hydrogen $n = 3$ state is approximately 10^{-8} s, and the average velocity of the hydrogen atoms is $< 10^5$ m/s. Thus, the distance traveled must be less than 0.001 m. A number of additional mechanisms have been proposed in order to explain the excessive Doppler broadening of the Balmer α line in argon-hydrogen DC or RF driven glow discharge plasmas all of which ultimately depend on electric field acceleration of hydrogen positive ions.

We recently reported a similar phenomenon for mixed gas plasmas containing hydrogen, but no argon: Preferential hydrogen line broadening, often extreme, was found in a number of

mixed gas discharge plasmas. Specifically, it has been reported that Balmer α lines broader than 0.25 nm were created in $He/H_2(10\%)$ as well as plasmas called resonant transfer (rt)-plasmas containing volatilized Sr such as Sr/H_2 and $Sr/He/H_2(10\%)$ plasmas which formed at 1000 K with extremely low or no electric field [8-17]. In none of these plasmas was there any significant broadening of the noble gas lines. Furthermore, hydrogen lines were not broadened in a number of other mixed gas plasmas including $Xe/H_2(10\%)$, and $Kr/H_2(10\%)$. These results show that the presence of hot hydrogen in mixed gas plasmas is not limited to Ar/H_2 . They also suggest, consistent with predictions [8-19], that only very special catalytic species will react in plasmas with hydrogen by a resonant, nonradiative energy transfer mechanism to generate hot hydrogen. Species such as He^+ , Ar^+ , and Sr^+ meet the catalyst criterion—a chemical or physical process with an enthalpy change equal to an integer multiple of $E_h = 27.2$ eV where E_h is one hartree. Catalyst are identifiable on the basis of their known electron energy levels. Conversely, species such as atoms or ions of Kr or Xe do not fulfill the criterion.

Recently there have been additional studies consistent with the model that some species act as catalysts (rt-plasma) for creating high energy H atoms in mixed gas plasmas. For example, in low pressure (0.5 Torr) $He/H_2(10\%)$ RF plasmas maintained in a GEC cell only the spectral lines of the H-atoms are Doppler broadened [19]. That is, there was no broadening at all of the He lines. Moreover, the hydrogen Balmer lines were broadened consistently to the same magnitude ~ 27 eV throughout the volume of the cell, and not simply in the region between the electrodes. The finding that the broadening was found throughout the volume indicated that earlier explanations for selective H-atom broadening in Ar/H_2 RF plasmas were not applicable. The earlier explanations all require that the origins of the Doppler energy is acceleration of H ions in the vicinity of the electrodes, even in cases where the excess broadening was found to be independent of position in the inter-electrode region [5-6].

Another finding in that study, also consistent with the rt-plasma model, was that in $Xe/H_2(10\%)$ plasmas there was no broadening of either hydrogen or Xe lines outside of the electrode region. Thus, it was argued that the broadening was consistent with a ‘chemical’ reaction occurring between He^+ and hydrogen species, throughout the volume of the cell. The magnitude the broadening was consistent with the magnitude of the energies of the initial and subsequent catalytic reactions that may be transferred to form fast, excited-state H [14-15, 20].

The average energy of the fast H was anticipated to depend on the particular catalyst as well as the conditions of the reaction. For oxygen, there are several chemical reactions that fulfill the catalyst criterion; thus, a mixed plasma with oxygen species may give an average H energy different from that of helium mixed plasmas under the same conditions. The bond energy of the oxygen molecule is 5.165 eV, and the first, second, and third ionization energies of an

oxygen atom are 13.61806 eV , 35.11730 eV , and 54.9355 eV , respectively [21]. The reactions $O_2 \rightarrow O + O^{2+}$, $O_2 \rightarrow O + O^{3+}$, and $2O \rightarrow 2O^+$ provide a net enthalpy of about 2, 4, and 1 times E_h , respectively [21]. It was previously reported that H lines were broadened and that both the Lyman and the Balmer α lines were observed to be inverted in certain rt-plasmas with oxygen catalyst [16-17, 22-23].

Our experiments on the measurement of the excited hydrogen atom energy in capacitively-coupled RF plasmas of H and catalyst O (both from decomposition of H_2O) or plasmas comprising hydrogen with noncatalyst xenon were also consistent with the rt-model. Direct mapping of the broadening of Balmer series lines for water plasmas in a GEC cell and the impact of applied power and operating pressure was studied for the first time. The results were once again supportive of a field-independent mechanism. In sum, the observation of position-independent excessive Balmer line broadening in an RF driven water-vapor plasmas is consistent with a model that predicts species such as oxygen [22-23], can act catalytically in plasma environments to create hot hydrogen atoms.

EXPERIMENTAL

Plasma Hardware- All plasmas were generated in a GEC-type cell [13] held at 0.5 Torr. This system, shown elsewhere [19], consisted of a large cylindrical (14 cm ID x 36 cm length) Pyrex chamber containing two parallel steel circular (8.25 cm diameter) plates, placed about 1 cm apart at the center. RF power from a RF VII, Model RF 5 13.6 MHz power supply was sent to the plates through 8 mm diameter steel feeds, which entered the chamber through standard Ultratorr fittings, one on each end of the chamber. UHP grade (99.999%) H_2 and Xe gases were metered into the chamber through Ultratorr fittings at one end, about 18 cm from the electrodes, using two mass flow controllers (MKS).

Water vapor was generated by pumping on a reservoir (about 20 cc) of distilled, deionized water. The flow rate was not directly controlled, but rather a needle valve was adjusted to maintain the desired pressure, as measured by a MKS Baratron placed above a Welch two-stage rotary vane oil-sealed vacuum pump (Model 8920) with a rated capacity of 218 l/min. This pump was attached to the chamber with a 1 cm ID Ultratorr fitting at the end opposite that at which gas entered. All parts, chamber, power supply, gauges, spectrometer, etc. were grounded with heavy-duty Reynolds aluminum foil to improve the magnitude of the signal to noise ratio.

Spectrometer- The spectrometer system used in this study, described in detail elsewhere [24], was built around a 1.25 m visible light instrument from Jobin Yvon-Spex with a holographic ruled diffraction grating (1800 g/mm), with a nearly flat response between 300 and 900 nm, and the slit was set at $10\text{ }\mu\text{m}$ in all cases. Light was collected using a light fiber bundle consisting of 19 fibers, each of $200\text{ }\mu\text{m}$ diameter, and a CCD for a detector. Light was input to

the spectrometer from the light fiber placed at position 1.) near the inlet end of the chamber approximately 15 cm from the cathode, 2.) in a quartz insert tube 1 cm in diameter that ended about 1 cm from the edge of the electrodes, or 3.) near the pump end of the chamber approximately 15 cm from the anode. The fiber was oriented ‘orthogonal’ relative to the azimuthal axis of the chamber in all cases. It is important to note that tests with a red laser with the system open clearly showed that light emanating from the region between the parallel-plate electrodes could not have reached the ‘hooded’ fiber optic probe when it was positioned at either end. Indeed, our tests showed that light no closer than 14 cm from the plate region reached the fiber optic probe at Positions 1 and 3. These readings were consistent with the listed 9° acceptance angle of the probe corresponding to a 1 cm diameter ‘spot’. Moreover, the probes were oriented such that the acceptance cone should ‘miss’ the power feeds by several centimeters.

In most cases, the data used for computations (e.g. excitation temperatures) was collected for the same time over the same wavelength region. Balmer series spectral lines were fit using three Gaussian curves: one for the ‘cold’ (<0.15 eV) hydrogen, one for ‘warm’ (<2 eV) hydrogen, and the third for ‘hot’ (>10 eV) hydrogen. It is notable that the fittings achieved were excellent, producing $R^2 > 0.98$ in all cases. One reason for the excellent fits was the absence of any signal in the relevant spectral region of the Balmer α and β lines of the water plasma (Figure 1a). In contrast, there was ‘signal’ in the same regions for the $Xe/H_2(10\%)$ plasma (Figure 1c).

RESULTS

A significant amount of data was collected in order to reliably detect trends in the H-atom line broadening in water plasmas as a function of plasma operating conditions. Data on line broadening was systematically collected for the Balmer α , β , γ , and δ lines at the three positions given in the Experimental section. Measured values of H-atom α and β line broadening for water plasmas at Positions 2 and 3, at ten or more pressures, and at three absorbed power levels (100 W, 150 W and 200 W), are presented in Tables I-VI. The data for the γ and δ lines is not presented as it is considered less reliable as the intensity of these lines is significantly lower. Also, the trends in Doppler energy of the hot hydrogen as a function of pressure and applied power is virtually identical to those observed from the α and β lines; thus, the data for the higher energy transitions in the Balmer series is regarded as somewhat redundant, and hence not essential to the arguments presented.

Typical peaks and the best fit of the data to three Gaussian curves corresponding to Doppler broadening are shown in Figure 1. All mechanisms other than Doppler would not produce a three component line, rather only a single component line.

The pressure dependence for a given adsorbed power plotted in Figures 2 and 3 shows that the energy of the hot hydrogen (as well as cold and warm atomic hydrogen) is independent of position. These same plots show that the Doppler energy of the hot hydrogen is strongly dependent on the pressure, dropping sharply above approximately 0.1 Torr in all cases. A comparison between the plots also suggests a weak dependence on the absorbed energy. In sum, the results reported here clearly show that there is ‘hot’ atomic hydrogen, of an apparent energy between 40 and 55 eV from the H_{α} line (approx. 450,000 to 550,000 K) and nearly 70 eV from the H_{β} line throughout GEC cell water vapor plasmas generated at low pressures (ca. < 0.08 Torr). No other species in these plasmas, specifically molecular hydrogen and various oxygen species, were found to be ‘hot’ at these low pressures.

Under all operating conditions the magnitude of the broadening at 15 cm from the electrodes was very close to the magnitude within the region between the plates. It is notable that the fraction of H-atoms that are hot is somewhat impacted by position within the cell. As shown in Figure 4, the fraction of ‘hot’ hydrogen is strongly dependent on pressure, and somewhat on adsorbed power, and is generally slightly higher between the plates than it is at the end of the cell, 15 cm from the electrodes.

Simple comparisons can be made between the results of this study of H_2O plasmas and earlier studies, performed in the same GEC cell, of He/H_2 plasmas [19]. First, it is notable that there is no overlap in the Doppler energies of the hot hydrogen measured for the two different plasmas, despite the fact that the physical arrangement of the cell (e.g. electrode separation) was virtually identical in both cases. For the water plasma the average broadening is always at least 10 eV greater than that found in the He/H_2 plasma. Also, one feature similar to that found with the He/H_2 plasma, is that the hydrogen concentration is asymmetric. For example, for the water plasmas it was consistently about twice as high at the ‘pump end’ (Position 3) as it is at the inlet end (Position 1). Although an exhaustive study of hydrogen lines was not made at Position 1, due to the low intensity of H-atom emission at that position, a limited number of comparisons were made, and it was clear that the magnitude of the line broadening, the average excitation, and other features were very nearly identical at both ends of the cell. Another difference: most (ca. 80%) of the atomic hydrogen was ‘hot’ in the He/H_2 plasma; whereas, less than half of the atomic hydrogen was found to be hot in the water plasma.

The intensities of all four Balmer lines were used to obtain a measure of the average hydrogen excitation temperature at Positions 2 and 3 as given in Figure 5 and Table VII. The excitation temperature was found to be around 0.5 ± 0.1 eV (approx. 5000 ± 1000 K) for all of the plasmas. This temperature was independent of the source of the different Balmer lines used in the computation within the error range: relative intensities of the cold, hot, or total hydrogen components of the Balmer lines. These values are also similar to electron temperatures

measured in earlier studies of low pressure Ar plasmas generated at slightly lower powers in a large glass cavity [25].

To test the catalyst mechanism, a control plasma, Xe/H_2 , was studied in some detail in this same GEC cell. Just as in the earlier studies with He/H_2 plasmas [19], these plasmas produced only narrow Balmer series lines (<2.5 eV) away from the electrodes and some ‘warm’ hydrogen (<3 eV) between the electrodes as shown in Figure 1C. In the earlier study [19], the ‘control’ plasma was run at pressures similar to those of the He/H_2 plasma studied, about 0.5 Torr. For this study, the control plasmas were studied at pressures close to those at which selective hydrogen broadening in a water plasma was observed (<0.9 Torr). The Balmer series line intensities in Xe/H_2 plasmas were very low even though the data collection times were four times greater than those for the water plasmas at matched pressures. Thus, it was necessary to run nearly pure H_2 to get sufficient signal at the low pressures employed in the present work.

DISCUSSION

In mixed gas plasmas containing argon and hydrogen, selective line broadening of atomic hydrogen lines (no broadening of lines belonging to argon or molecular hydrogen) in high field regions [1-7, 26-28] has been reported repeatedly. Even in pure hydrogen plasmas, generated with DC discharge or RF systems, including one group using a GEC cell [7], selective broadening of atomic hydrogen lines has been reported.

All groups agree that the broadening of the lines is Doppler in origin. Stark broadening can be eliminated because the required electron densities are orders of magnitude greater than the gas densities. Moreover, the lines are composed of three parts: hot, warm and cold. All H atoms, not just a fraction, as well as other species, would be impacted by high charge densities. Optical thickness cannot be a factor by the same argument: the entire line would be broadened, not just a fraction. Computation also shows that the optical thickness cannot be a factor. Specifically, for optically thin plasmas (self adsorption not significant), the effective path length $\tau_\omega(L)$ is less than one:

$$\tau_\omega(L) = \sigma_\omega N_H L < 1 \quad (1)$$

where σ_ω is the absorption cross section, N_H is the number density, and L is the plasma path length traversed by the light. The absorption cross section for Balmer α emission is $\sigma = 1 \times 10^{-16} \text{ cm}^2$ [29]. An upper limit on the excited H_α density, assuming all of the water is fully dissociated, the temperature (as measured) is 5000 K, and, the excited states are populated according to the Boltzmann distribution (as measured), is 10^3 cm^{-3} . No more than 15 cm of plasma is traversed. Putting these values together yields an effective path length of the order 10^{-12} cm . Clearly, these plasmas are optically thin. Other potential explanations such as instrument broadening can be readily eliminated because those mechanisms would not produce

selective broadening of one species. Moreover, all the Balmer series lines are broadened approximately to the same energy level, a result completely consistent with Doppler broadening.

All of the above arguments apply to the line broadening observed in the present work. Thus, we conclude that some of the hydrogen atoms (between 10 and 45 percent, Figure 4) in the water plasma are selectively ‘heated’ to extremely high temperatures, 450,000 to 700,000 K. About half of the remaining hydrogen (‘cold’) produces line broadening consistent not with a Doppler effect, but rather with a combination of Stark effect, instrument effects, etc. A third type of hydrogen (‘warm’) may be due to a catalytic effect of hydrogen alone when maintained in high concentration such found on the surface of the cathode as reported previously [9, 13].

The standard physics models for the generation of the hot hydrogen in Ar/H_2 plasmas all include the requirement that the hydrogen ions obtain energy directly from the field [1-7, 26-28]. The possibility that the hot hydrogen forms from collisions with hot gas species (ions or atoms) is considered highly unlikely. First, the cross sections for collisions with H ions are too small, second spectroscopy indicates there is little or no hot argon of any form present [27]. Thus, the selective H broadening is explained only in terms of acceleration of charged H species. In fact, there are two classes of models: 1.) those postulating a gas phase mechanism involving formation of hot hydrogen near the electrodes, and 2.) those requiring that an H ionic species hits the electrode resulting in energy transfer to absorbed hydrogen species and consequently the desorption of a hot hydrogen atom. In the ‘bombardment’ models hydrogen species on electrode surfaces are ‘hit’ by energized ions, generally H_3^+ , H_2^+ , or H^+ ions [3, 27], and subsequently ejected as hot hydrogen [27-28]. In all cases, these models only predict selective hydrogen broadening in high field regions. In the gas production model, a hydrogen ion such as H_3^+ [3] that is increased in concentration by interactions of H_2 with Ar , is accelerated by the field toward an electrode, captures an electron via interaction with an Ar , dissociates to form n=3 state hydrogen, or forms n=3 state hydrogen via collision with a neutral Ar [27], and then emits.

There does not appear to be any variation on those standard physics models capable of explaining the observations of the present work. First, hot hydrogen was found throughout the chamber rather than only in the vicinity of the electrodes. Hot hydrogen ions created near the electrodes simply cannot migrate 15 cm without equilibrating with the plasma gas. Given a maximum computed mean free path of the hot hydrogen of 10^{-4} cm at 0.1 Torr, the high temperature would have to remain undiminished through 10^5 collisions to be observed at 15 cm distance from the electrode. The excitation temperature of the ‘parent’ atomic hydrogen species was only about 5000 K (approximately 0.5 eV), and as the excitation temperature of RF plasmas is generally associated with the electron temperature [30-32]. This means that the internal temperature of the atomic hydrogen, as well as the temperature of the electrons in the plasma, were about two orders of magnitude lower than that of the hot hydrogen. Thus, any conventional

model must explain how H atoms can be two orders of magnitude hotter than the electrons in the GEC plasmas studied.

Even relatively obscure postulated processes were considered as mechanisms to provide the observed energy of the hot hydrogen atoms. For example, the ‘Frank-Condon’ effect [33-37] will create ‘hot’ neutrals with energies between 2 and 4.5 eV via wall reactions of the type:



Clearly, the energy of neutral species created in this fashion do not match the energies of the neutrals observed in this study.

In sum, it is untenable to suggest modifications of the earlier models can explain the present data. For example, all earlier models require acceleration of ions in the high field (unscreened) regions near the electrodes. The earlier models also include other specific predictions, such as preferential population of $n=3$ states, which are not observed. The gas phase models must be rejected for two additional reasons. First, they all require a high cross section for charge transfer, peculiar to argon and hydrogen ions, to allow for the rapid charge transfer necessary to create neutral, high energy H_2 , which must be formed before high energy (neutral) H atoms can form. There was no argon in the plasmas studied for this work. Second, the H_2 lines were not observed to be broadened. Third, it is not plausible to suggest that the fields found 15 cm from the electrode are as strong as those found in the boundary layer near the electrodes. Field screening by the sheath reduces the fields dramatically within millimeters, and a highly conductive plasma bulk is essentially equipotential [6]. Yet, the hot hydrogen found at 15 cm from the electrodes was of the same energy as that found between the electrodes. This third objection to the gas phase models clearly also shows the ‘bombardment’ models to be implausible. Indeed, how can a hot hydrogen atom generated at the electrode by bombardment traverse 15 cm of the plasma without loosing energy or thermalizing? Clearly, the electrode bombardment models are not consistent with the finding of the present study that the degree of broadening was the same throughout the plasma volume.

Moreover, we cannot identify any previously proposed mechanism that can produce hydrogen atoms with an average energy of about 45 eV for the water plasma, nearly twice the average energy observed for He/H_2 plasmas generated in an identical system [19]. Why is this process completely absent in the Xe/H_2 plasmas? What ‘energy from the field’ process would produce neutrals with energies two orders of magnitude higher than those of the electrons in the plasma?

These results extend the list of successfully predicted rt-plasma catalysts [8-20, 22-23, 26-30, 38-40] to include oxygen which under the studied conditions produces more energetic H than He^+ [19]. Under plasma discharge [41-44] and the inherent photolysis conditions [45] water is known to undergo decomposition to primarily hydrogen atoms and hydroxyl radials, and

the hydroxyl radicals can further form hydrogen and oxygen atoms. The oxygen can serve as a catalyst for atomic hydrogen to release EUV light and fast H as reported previously [22, 46]. The energy released is sufficient to account for the observed excitation and Doppler energies.

The catalysis reaction requires atomic hydrogen and atomic or molecular oxygen. These species are favored to form at low pressures, which is consistent with the observed pressure dependence. The pressure dependence could also be explained somewhat by field acceleration, but it can not explain why only the hydrogen lines are broadened at low pressure, and Stark broadening would be anticipated at high pressure, the opposite of the observed dependency.

Only the rt-plasma mechanism is consistent with all of the observations. Since additional such reactions of varying energies are possible as discussed previously [14-15, 20], the particular conditions in the cell may favor more than one H population. Collisional energy transfer between fast H and matrix gas may also give rise to a bimodal or trimodal distribution.

REFERENCES

1. M. Kuraica, N. Konjevic, "Line shapes of atomic hydrogen in a plane-cathode abnormal glow discharge," *Physical Review A*, Volume 46, No. 7, October (1992), pp. 4429-4432.
2. M. Kuraica, N. Konjevic, M. Platisa and D. Pantelic, *Spectrochimica Acta* Vol. 47, 1173 (1992).
3. I. R. Videnovic, N. Konjevic, M. M. Kuraica, "Spectroscopic investigations of a cathode fall region of the Grimm-type glow discharge," *Spectrochimica Acta, Part B*, Vol. 51, (1996), pp. 1707-1731.
4. S. Alexiou, E. Leboucher-Dalimier, "Hydrogen Balmer- α in dense plasmas," *Phys. Rev. E*, Vol. 60, No. 3, (1999), pp. 3436-3438.
5. S. Djurovic, J. R. Roberts, "Hydrogen Balmer alpha line shapes for hydrogen-argon mixtures in a low-pressure rf discharge," *J. Appl. Phys.*, Vol. 74, No. 11, (1993), pp. 6558-6565.
6. S. B. Radovanov, K. Dzierzega, J. R. Roberts, J. K. Olthoff, Time-resolved Balmer-alpha emission from fast hydrogen atoms in low pressure, radio-frequency discharges in hydrogen," *Appl. Phys. Lett.*, Vol. 66, No. 20, (1995), pp. 2637-2639.
7. S. B. Radovanov, J. K. Olthoff, R. J. Van Brunt, S. Djurovic, "Ion kinetic-energy distributions and Balmer-alpha (H_{α}) excitation in $Ar - H_2$ radio-frequency discharges," *J. Appl. Phys.*, Vol. 78, No. 2, (1995), pp. 746-757.
8. R. L. Mills, P. Ray, "Substantial Changes in the Characteristics of a Microwave Plasma Due to Combining Argon and Hydrogen," *New Journal of Physics*, www.njp.org, Vol. 4, (2002), pp. 22.1-22.17.
9. R. L. Mills, P. Ray, B. Dhandapani, R. M. Mayo, J. He, "Comparison of Excessive Balmer α Line Broadening of Glow Discharge and Microwave Hydrogen Plasmas with Certain

Catalysts," J. of Applied Physics, Vol. 92, No. 12, (2002), pp. 7008-7022.

- 10. R. Mills and M. Nansteel, P. Ray, "Argon-Hydrogen-Strontium Discharge Light Source," IEEE Transactions on Plasma Science, Vol. 30, No. 2, (2002), pp. 639-653.
- 11. R. Mills, M. Nansteel, and P. Ray, "Excessively Bright Hydrogen-Strontium Plasma Light Source Due to Energy Resonance of Strontium with Hydrogen," J. of Plasma Physics, Vol. 69, (2003), pp. 131-158.
- 12. R. Mills and M. Nansteel, P. Ray, "Bright Hydrogen-Light Source due to a Resonant Energy Transfer with Strontium and Argon Ions," New Journal of Physics, Vol. 4, (2002), pp. 70.1-70.28.
- 13. R. L. Mills, P. Ray, B. Dhandapani, J. He, "Comparison of Excessive Balmer α Line Broadening of Inductively and Capacitively Coupled RF, Microwave, and Glow Discharge Hydrogen Plasmas with Certain Catalysts," IEEE Transactions on Plasma Science, Vol. 31, No. (2003), pp. 338-355.
- 14. R. L. Mills, P. Ray, "Extreme Ultraviolet Spectroscopy of Helium-Hydrogen Plasma," J. Phys. D, Applied Physics, Vol. 36, (2003), pp. 1535-1542.
- 15. R. L. Mills, P. Ray, B. Dhandapani, M. Nansteel, X. Chen, J. He, "New Power Source from Fractional Quantum Energy Levels of Atomic Hydrogen that Surpasses Internal Combustion," J Mol. Struct., Vol. 643, No. 1-3, (2002), pp. 43-54.
- 16. R. Mills, P. Ray, R. M. Mayo, "CW H I Laser Based on a Stationary Inverted Lyman Population Formed from Incandescently Heated Hydrogen Gas with Certain Group I Catalysts," IEEE Transactions on Plasma Science, Vol. 31, No. 2, (2003), pp. 236-247.
- 17. R. L. Mills, P. Ray, "Stationary Inverted Lyman Population Formed from Incandescently Heated Hydrogen Gas with Certain Catalysts," J. Phys. D, Applied Physics, Vol. 36, (2003), pp. 1504-1509.
- 18. R. Mills, J. Dong, Y. Lu, "Observation of Extreme Ultraviolet Hydrogen Emission from Incandescently Heated Hydrogen Gas with Certain Catalysts," Int. J. Hydrogen Energy, Vol. 25, (2000), pp. 919-943.
- 19. J. Phillips, C. Chen, "Evidence of Energetic Reaction Between Helium and Hydrogen Species in RF Generated Plasmas," submitted.
- 20. R. Mills, P. Ray, "Spectral Emission of Fractional Quantum Energy Levels of Atomic Hydrogen from a Helium-Hydrogen Plasma and the Implications for Dark Matter," Int. J. Hydrogen Energy, Vol. 27, No. 3, pp. 301-322.
- 21. D. R. Lide, CRC Handbook of Chemistry and Physics, 79 th Edition, CRC Press, Boca Raton, Florida, (1998-1999), p. 9-55 and p. 10-175.
- 22. R. Mills, P. Ray, R. M. Mayo, "The Potential for a Hydrogen Water-Plasma Laser," Applied Physics Letters, Vol. 82, No. 11, (2003), pp. 1679-1681.

23. R. L. Mills, P. C. Ray, R. M. Mayo, M. Nansteel, B. Dhandapani, J. Phillips, "Spectroscopic Study of Unique Line Broadening and Inversion in Low Pressure Microwave Generated Water Plasmas," submitted.

24. C. K. Chen and J. Phillips, *J. Phys. D: Applied Physics*, **35**, 998-1009 (2002).

25. D. Barton, J. W. Bradley, D. A. Steele, and R. D. Short, "Investigating radio frequency plasmas used for the modification of polymer surfaces," *J. Phys. Chem. B*, Vol. 103, (1999), pp. 4423-4430.

26. G. Baravian, Y. Chouan, A. Ricard, and G. Sultan, *J. Appl. Phys.* **61**, 5249 (1987).

27. E. L. Ayers and W. Benesch, *Phys. Rev.* **A37**, 194 (1988).

28. A. V. Phelps, *J. Phys. Chem. Ref Data* **21**, 883 (1992).

29. H. Okabe, *Photochemistry of Small Molecules*, John Wiley & Sons, New York, (1978).

30. H. R. Griem, *Plasma Spectroscopy*, (McGraw-Hill, New York, 1964).

31. P. W. J. M. Boumans, "Excitation Spectra" in *Analytical Emission Spectrometry*, (E. L. Grove, Ed., Dekker, New York, 1972).

32. A. P. Thorne, *Spectroscophysics*, (Chapman and Hall, London, 1974).

33. H. Conrads, R. Mills, Th. Wrubel, "Emission in the Deep Vacuum Ultraviolet from a Plasma Formed by Incandescently Heating Hydrogen Gas with Trace Amounts of Potassium Carbonate," *Plasma Sources Science and Technology*, Vol. 12, (2003), pp. 389-395.

34. J. A. M. van der Mullen, *Spectrochim. Acta*, **45B**, 1 (1990).

35. D. R. Sweetman, *Phys. Rev. Lett.* **3**, 425 (1959).

36. D. R. Sweetman, *Proc. Phys. Soc. Lon.* **78**, 1215 (1961).

37. D. R. Sweetman, *Proc. R. Soc. Lon. A* **256**, 416 (1960).

38. R. Mills, P. Ray, "Vibrational Spectral Emission of Fractional-Principal-Quantum-Energy-Level Hydrogen Molecular Ion," *Int. J. Hydrogen Energy*, Vol. 27, No. 5, (2002), pp. 533-564.

39. R. L. Mills, P. Ray, J. Dong, M. Nansteel, B. Dhandapani, J. He, "Spectral Emission of Fractional-Principal-Quantum-Energy-Level Atomic and Molecular Hydrogen," *Vibrational Spectroscopy*, Vol. 31, No. 2, (2003), pp. 195-213.

40. R. Mills, B. Dhandapani, M. Nansteel, J. He, T. Shannon, A. Echezuria, "Synthesis and Characterization of Novel Hydride Compounds," *Int. J. of Hydrogen Energy*, Vol. 26, No. 4, (2001), pp. 339-367.

41. A. Crocker, H. A. Gebbie, M. F. Kimmitt, L. E. S. Mathias, "Stimulated emission in the far infra-red," *Nature*, Vol. 201, (1964), pp. 250-251.

42. W. J. Sarjeant, Z. Kucerovsky, E. Brannen, "Excitation processes and relaxation rates in the pulsed water vapor laser," *Applied Optics*, Vol. 11, No. 4, (1972), pp. 735-741.

43. A. K. Shuaibov, A. I. Dashchenko, I. V. Shevera, "Stationary radiator in the 130-190 nm

range based on water vapour plasma," Quantum Electronics, Vol. 31, No. 6, (2001), pp. 547-548.

44. A. K. Shuaibov, L. L. Shimon, A. I. Dashchenko, I. V. Shevera, "Optical characteristics of a glow discharge in a He/H_2O mixture," Plasma Physics Reports, Vol. 27, No. 10, (2001), pp. 897-900.

45. J. C. Calvert, J. N. Pitts, *Photochemistry*, John Wiley & Sons, New York, (1966), p. 200.

46. R. L. Mills, P. Ray, R. M. Mayo, "Highly Pumped Inverted Balmer and Lyman Populations," submitted.

Table 1. Analysis of H α lines in 100 W water plasmas

RF Power = 100W	Position / Balmer Lines	Pressure (torr)	Doppler Energy Cold H (eV)	Doppler Energy Warm H (eV)	Doppler Energy Hot H (eV)	Area Ratio Hot/All
2 / H α	2 / H α	0.23	0.122	1.336	11.6	0.250
	2 / H α	0.19	0.123	1.373	10.8	0.269
	2 / H α	0.17	0.122	1.412	11.0	0.288
	2 / H α	0.15	0.123	1.470	11.8	0.287
	2 / H α	0.13	0.124	1.502	12.6	0.291
	2 / H α	0.12	0.122	1.459	12.5	0.303
	2 / H α	0.10	0.121	1.475	14.1	0.287
	2 / H α	0.09	0.121	1.517	16.2	0.263
	2 / H α	0.08	0.119	1.560	23.1	0.245
	2 / H α	0.07	0.118	1.517	35.0	0.245
	2 / H α	0.06	0.117	1.291	37.9	0.252
	2 / H α	0.05	0.116	1.193	39.2	0.251
	2 / H α	0.04	0.114	1.195	42.1	0.218
	2 / H α	0.03	0.114	1.360	42.4	0.159
	2 / H α	0.02	0.104	1.539	37.3	0.078
3 / H α	3 / H α	0.18	0.124	1.043	8.2	0.135
	3 / H α	0.17	0.118	1.124	12.4	0.137
	3 / H α	0.15	0.122	1.136	15.1	0.127
	3 / H α	0.13	0.117	1.176	23.2	0.133
	3 / H α	0.11	0.120	1.244	20.7	0.126
	3 / H α	0.09	0.118	1.218	19.1	0.141
	3 / H α	0.08	0.118	1.261	34.4	0.136
	3 / H α	0.07	0.116	1.263	23.3	0.135
	3 / H α	0.06	0.118	1.371	29.7	0.156
	3 / H α	0.05	0.115	1.350	37.1	0.211
	3 / H α	0.04	0.115	1.252	37.6	0.250
	3 / H α	0.03	0.113	1.432	32.2	0.083

Table 2. Analysis of H α lines in 150 W water plasmas

RF Power = 150W	Position / Balmer Lines	Pressure (torr)	Doppler Energy Cold H (eV)	Doppler Energy Warm H (eV)	Doppler Energy Hot H (eV)	Area Ratio Hot/All
2 / H α	2 / H α	0.20	0.126	1.497	12.7	0.258
	2 / H α	0.17	0.121	1.446	12.6	0.294
	2 / H α	0.15	0.123	1.536	14.0	0.300
	2 / H α	0.13	0.123	1.600	15.9	0.294
	2 / H α	0.11	0.119	1.478	17.1	0.304
	2 / H α	0.09	0.118	1.562	27.1	0.281
	2 / H α	0.08	0.119	1.594	43.7	0.303
	2 / H α	0.07	0.117	1.404	44.1	0.358
	2 / H α	0.06	0.117	1.110	48.9	0.345
	2 / H α	0.04	0.117	1.163	49.0	0.278
	2 / H α	0.03	0.113	1.323	52.1	0.203
	2 / H α	0.02	0.111	1.687	50.7	0.145
3 / H α	3 / H α	0.20	0.119	1.161	19.1	0.159
	3 / H α	0.18	0.124	1.250	25.5	0.148
	3 / H α	0.15	0.126	1.167	20.9	0.160
	3 / H α	0.13	0.119	1.262	24.4	0.165
	3 / H α	0.11	0.118	1.325	23.5	0.145
	3 / H α	0.09	0.115	1.410	43.7	0.189
	3 / H α	0.08	0.116	1.554	41.5	0.277
	3 / H α	0.07	0.117	1.404	44.4	0.359
	3 / H α	0.05	0.115	1.378	45.2	0.335
	3 / H α	0.04	0.117	1.376	43.6	0.260

Table 3. Analysis of H α lines in 200 W water plasmas

RF Power = 200W	Position / Balmer Lines	Pressure (torr)	Doppler Energy Cold H (eV)	Doppler Energy Warm H (eV)	Doppler Energy Hot H (eV)	Area Ratio Hot/All
2 / H α	0.22	0.123	1.369	11.6	0.268	
	0.18	0.125	1.459	12.4	0.296	
	0.15	0.122	1.520	14.3	0.313	
	0.13	0.122	1.618	17.5	0.310	
	0.12	0.121	1.668	23.7	0.306	
	0.11	0.119	1.605	36.3	0.307	
	0.09	0.115	1.295	51.6	0.414	
	0.07	0.117	1.174	52.1	0.432	
	0.05	0.116	1.142	52.0	0.350	
	0.04	0.116	1.252	53.3	0.260	
	0.03	0.110	1.585	53.2	0.159	
3 / H α	0.21	0.119	1.108	13.9	0.171	
	0.17	0.121	1.149	14.3	0.172	
	0.13	0.123	1.158	15.0	0.181	
	0.11	0.124	1.225	20.7	0.188	
	0.09	0.119	1.252	23.2	0.204	
	0.08	0.120	1.370	31.2	0.203	
	0.08	0.117	1.490	44.8	0.256	
	0.07	0.116	1.421	50.4	0.412	
	0.05	0.116	1.352	50.6	0.421	
	0.04	0.115	1.432	47.4	0.244	
	0.03	0.122	2.045	x	0.000	

Table 4. Analysis of H β lines in 100 W water plasmas

RF Power = 100W	Position / Balmer Lines	Pressure (torr)	Doppler Energy Cold H (eV)	Doppler Energy Warm H (eV)	Doppler Energy Hot H (eV)	Area Ratio Hot/All
2 / H β	2 / H β	0.21	0.143	1.644	11.0	0.203
2 / H β	2 / H β	0.17	0.156	1.936	25.7	0.172
2 / H β	2 / H β	0.16	0.239	2.480	14.7	0.175
2 / H β	2 / H β	0.14	0.132	1.820	19.7	0.216
2 / H β	2 / H β	0.12	0.142	1.944	18.4	0.198
2 / H β	2 / H β	0.11	0.175	3.331	17.0	0.148
2 / H β	2 / H β	0.10	0.134	1.841	13.9	0.219
2 / H β	2 / H β	0.08	0.127	1.699	22.6	0.193
2 / H β	2 / H β	0.07	0.127	1.730	28.6	0.207
2 / H β	2 / H β	0.06	0.128	1.679	38.8	0.219
2 / H β	2 / H β	0.05	0.129	1.679	39.5	0.176
2 / H β	2 / H β	0.04	0.128	1.648	46.8	0.148
2 / H β	2 / H β	0.03	0.110	1.698	22.4	0.070
3 / H β	3 / H β	0.20	0.138	1.191	5.7	0.142
3 / H β	3 / H β	0.16	0.145	1.421	8.2	0.104
3 / H β	3 / H β	0.14	0.137	1.324	5.3	0.030
3 / H β	3 / H β	0.12	0.138	1.454	26.6	0.107
3 / H β	3 / H β	0.10	0.132	1.367	12.0	0.099
3 / H β	3 / H β	0.09	0.127	1.396	6.9	0.099
3 / H β	3 / H β	0.08	0.123	1.446	14.2	0.124
3 / H β	3 / H β	0.07	0.126	1.505	11.5	0.111
3 / H β	3 / H β	0.06	0.120	1.810	52.3	0.251
3 / H β	3 / H β	0.05	0.122	1.890	58.9	0.176
3 / H β	3 / H β	0.03	0.122	1.728	63.4	0.092

Table 5. Analysis of H β lines in 150 W water plasmas

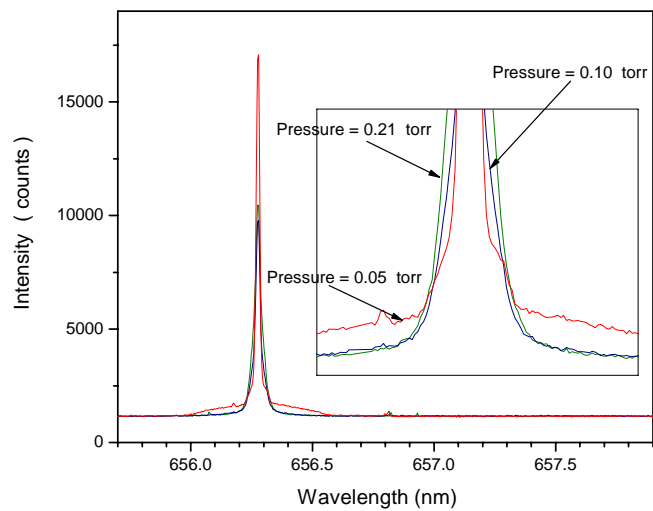
RF Power = 150W	Position / Balmer Lines	Pressure (torr)	Doppler Energy Cold H (eV)	Doppler Energy Warm H (eV)	Doppler Energy Hot H (eV)	Area Ratio Hot/All
2 / H $_{\beta}$	2 / H $_{\beta}$	0.23	0.139	1.840	21.9	0.197
	2 / H $_{\beta}$	0.17	0.122	1.711	11.9	0.268
	2 / H $_{\beta}$	0.15	0.130	2.033	26.0	0.224
	2 / H $_{\beta}$	0.13	0.123	2.011	28.7	0.193
	2 / H $_{\beta}$	0.11	0.131	2.020	34.5	0.241
	2 / H $_{\beta}$	0.10	0.129	1.887	36.9	0.273
	2 / H $_{\beta}$	0.08	0.127	1.643	43.2	0.331
	2 / H $_{\beta}$	0.07	0.126	1.580	50.6	0.338
	2 / H $_{\beta}$	0.06	0.127	1.643	54.5	0.258
	2 / H $_{\beta}$	0.06	0.126	1.579	41.9	0.199
	2 / H $_{\beta}$	0.05	0.110	1.780	31.4	0.084
3 / H $_{\beta}$	3 / H $_{\beta}$	0.22	0.136	1.359	21.0	0.115
	3 / H $_{\beta}$	0.18	0.116	1.325	13.6	0.123
	3 / H $_{\beta}$	0.15	0.140	1.515	18.6	0.069
	3 / H $_{\beta}$	0.13	0.129	1.639	27.9	0.063
	3 / H $_{\beta}$	0.11	0.131	1.647	33.2	0.106
	3 / H $_{\beta}$	0.09	0.121	1.747	27.1	0.120
	3 / H $_{\beta}$	0.08	0.113	1.898	39.8	0.181
	3 / H $_{\beta}$	0.07	0.118	1.881	43.3	0.284
	3 / H $_{\beta}$	0.05	0.120	1.746	53.0	0.338
	3 / H $_{\beta}$	0.04	0.120	1.850	49.9	0.304
	3 / H $_{\beta}$	0.03	0.122	1.836	45.6	0.119

Table 6. Analysis of H β lines in 200 W water plasmas

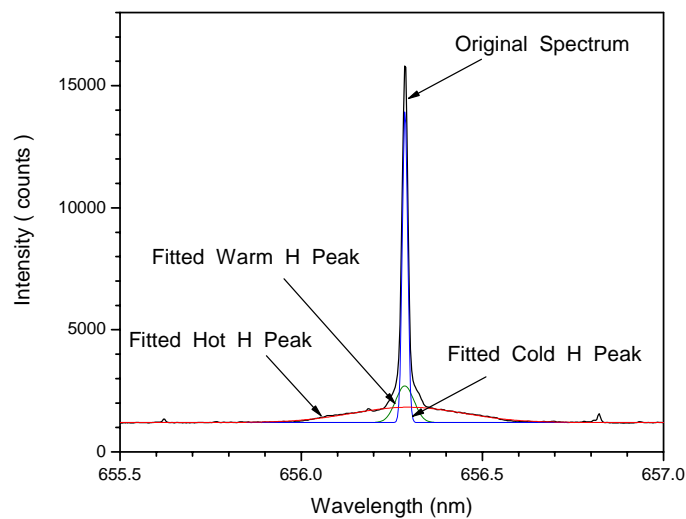
RF Power = 200W	Position / Balmer Lines	Pressure (torr)	Doppler Energy Cold H (eV)	Doppler Energy Warm H (eV)	Doppler Energy Hot H (eV)	Area Ratio Hot/All
	2 / H $_{\beta}$	0.22	0.131	1.734	13.6	0.228
	2 / H $_{\beta}$	0.18	0.127	1.920	21.1	0.223
	2 / H $_{\beta}$	0.16	0.129	1.930	23.9	0.247
	2 / H $_{\beta}$	0.14	0.125	2.046	33.4	0.226
	2 / H $_{\beta}$	0.12	0.100	1.901	35.2	0.257
	2 / H $_{\beta}$	0.10	0.123	1.913	29.7	0.219
	2 / H $_{\beta}$	0.08	0.126	1.870	42.2	0.311
	2 / H $_{\beta}$	0.07	0.129	1.837	52.7	0.341
	2 / H $_{\beta}$	0.05	0.139	1.471	46.7	0.380
	2 / H $_{\beta}$	0.04	0.125	1.594	58.9	0.308
	2 / H $_{\beta}$	0.03	0.113	1.740	54.5	0.164
	3 / H $_{\beta}$	0.15	0.124	1.550	25.1	0.152
	3 / H $_{\beta}$	0.13	0.120	1.719	39.8	0.174
	3 / H $_{\beta}$	0.11	0.122	1.812	52.0	0.208
	3 / H $_{\beta}$	0.09	0.122	1.917	62.7	0.383
	3 / H $_{\beta}$	0.07	0.121	1.750	61.4	0.479
	3 / H $_{\beta}$	0.05	0.120	1.793	54.5	0.425
	3 / H $_{\beta}$	0.04	0.122	1.877	56.3	0.400
	3 / H $_{\beta}$	0.03	0.119	1.700	42.0	0.251
	3 / H $_{\beta}$	0.02	0.127	1.549	15.3	0.156

FIGURE 1. Hydrogen Balmer α lines indicate presence of hydrogen atoms with energy in excess of 40 eV. (a) At 0.08 Torr, 150 W, Position 3, Doppler broadening from H atoms with energies greater than 40 eV is seen at the base of the H α peak. No ‘hot’ hydrogen is seen at higher pressures. (b) Fitting the lines requires three peaks, for ‘cold’ (<1 eV), ‘warm’ (<2.5 eV) and ‘hot’ hydrogen. (c) Between the electrodes in control plasmas (150 W, 0.05 Torr, H₂/Xe,20:1) only cold and warm hydrogen are found. Away from the electrode region only cold hydrogen is present.

(a)



(b)



(c)

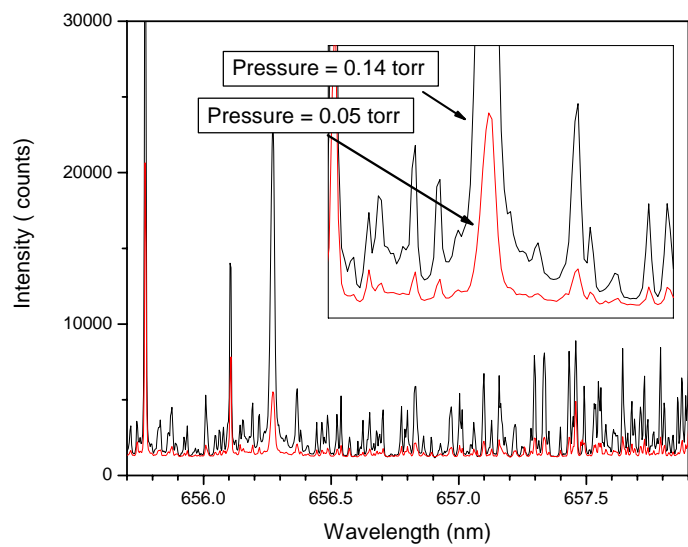
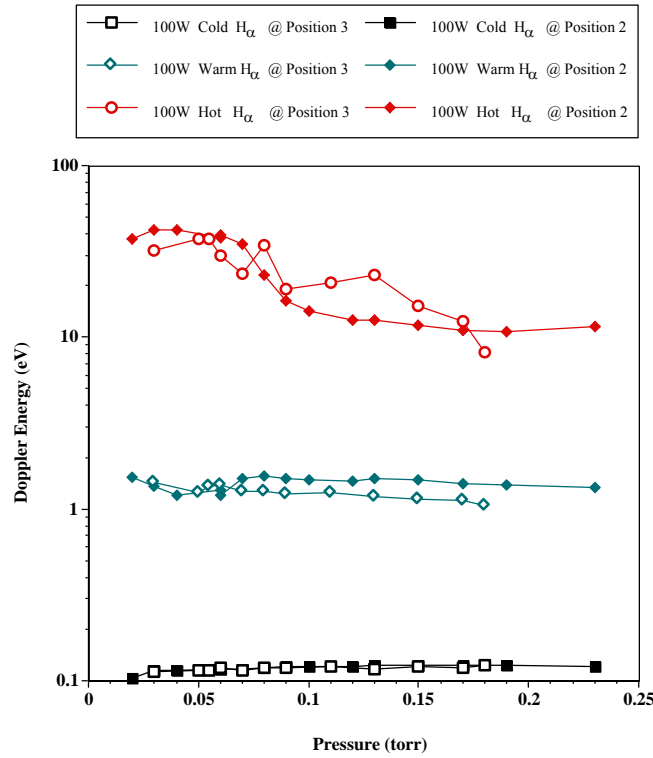
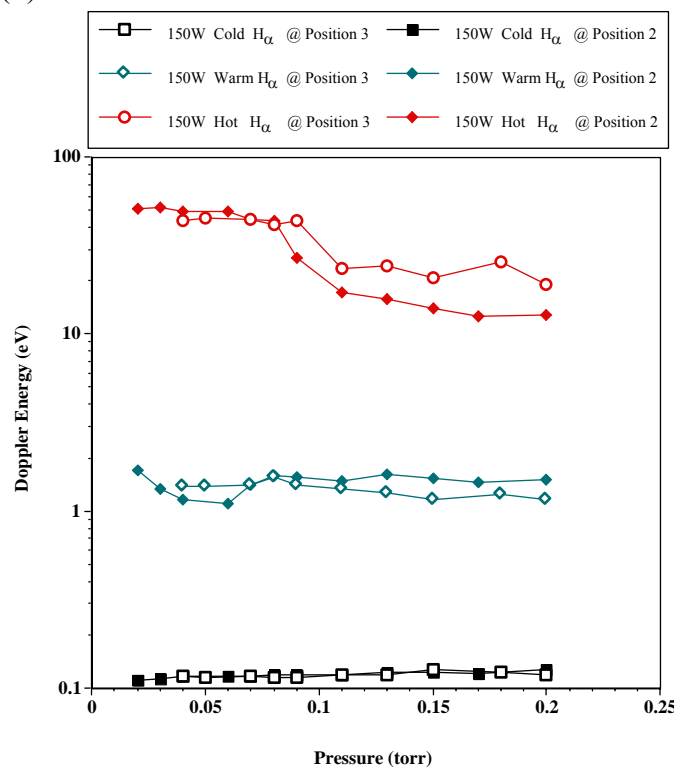


FIGURE 2. $H\alpha$ broadening indicates ‘hot’ atomic hydrogen energy a function of pressure but not position. (a) At 100 W the broadening is approximately 40 eV up to a pressure of 0.08 Torr. (b) At 150 W the measured broadening is approximately 45 eV up to a pressure of about 0.08 Torr. (c) At 200 W the measured broadening is above 45 eV up to a pressure of nearly 0.10 Torr. In all cases the ‘warm’ hydrogen is less than 2eV and the ‘cold’ hydrogen line width is so small it probably reflects factors (natural line width, Stark effect, instrument effects, etc.) other than Doppler broadening. Also note that the ‘hot’ hydrogen Doppler energy drops to between 10 and 20 eV at pressures above 0.10 Torr.

(a)



(b)



(c)

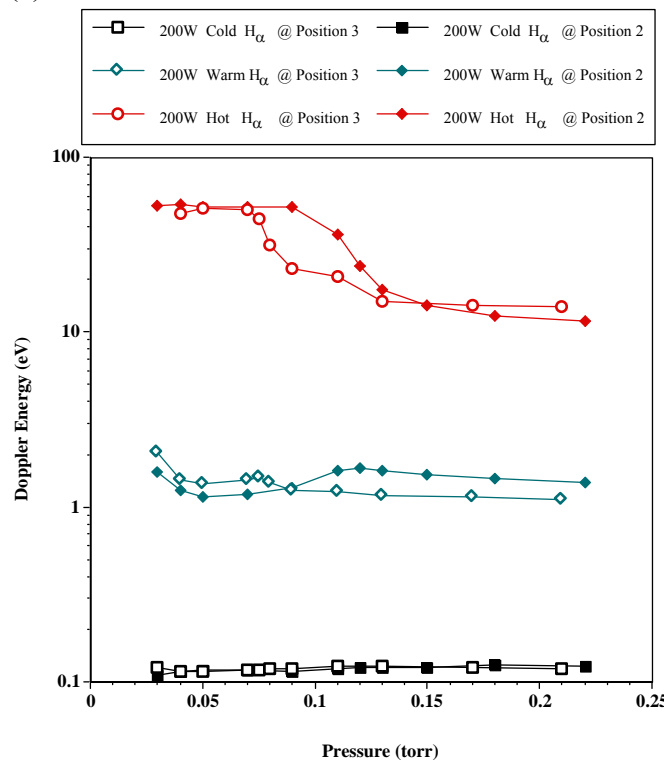
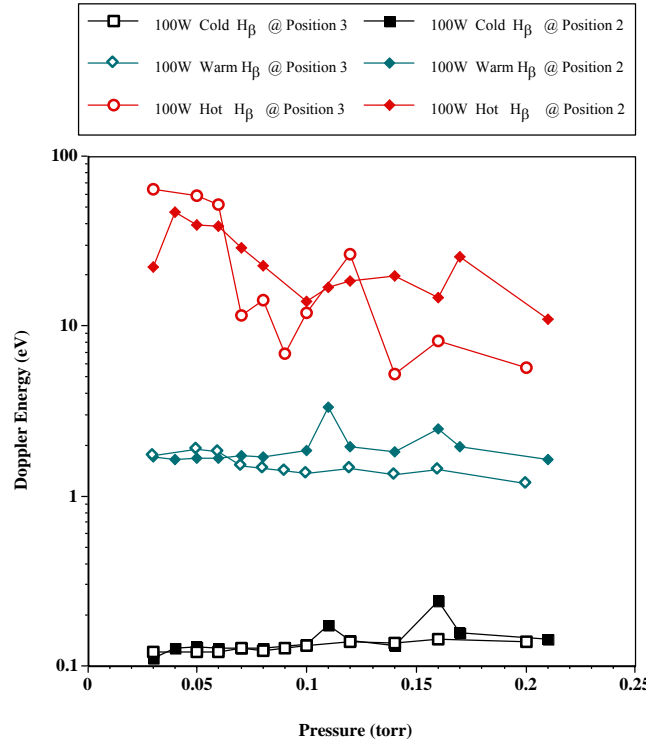
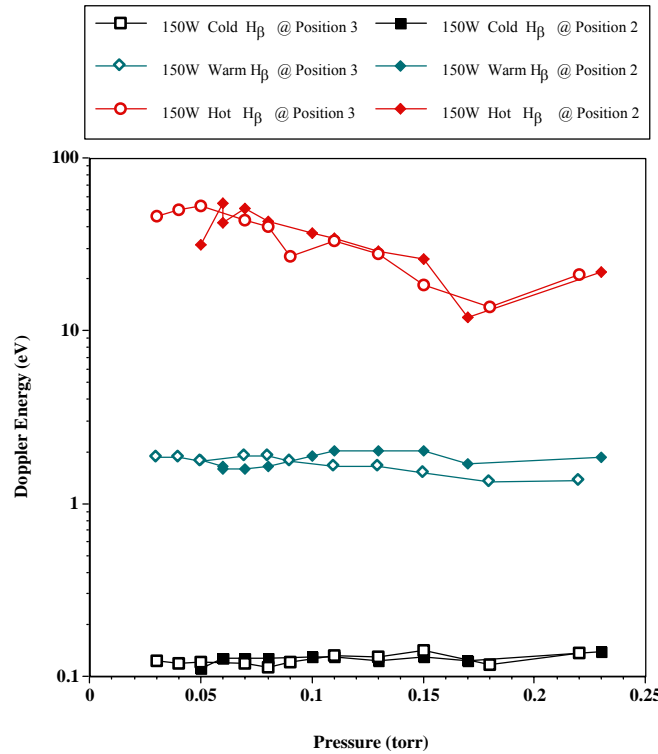


FIGURE 3. H β broadening also indicates ‘hot’ atomic hydrogen energy a function of pressure, but not position. (a) At 100 W the broadening is greater than 40 eV up to a pressure of 0.06 Torr. (b) At 150 W the measured broadening is greater than 40 eV up to a pressure of about 0.09 Torr. (c) At 200 W the measured broadening is above 40 eV up to a pressure of nearly 0.10 Torr. In all cases the ‘warm’ hydrogen is less than 2eV and the ‘cold’ hydrogen line width is so small it probably reflects factors (natural line width, Stark effect, instrument effects, etc.) other than Doppler broadening. Also note that the ‘hot’ hydrogen Doppler energy drops to between 10 and 20 eV at pressures above 0.10 Torr.

(a)



(b)



(c)

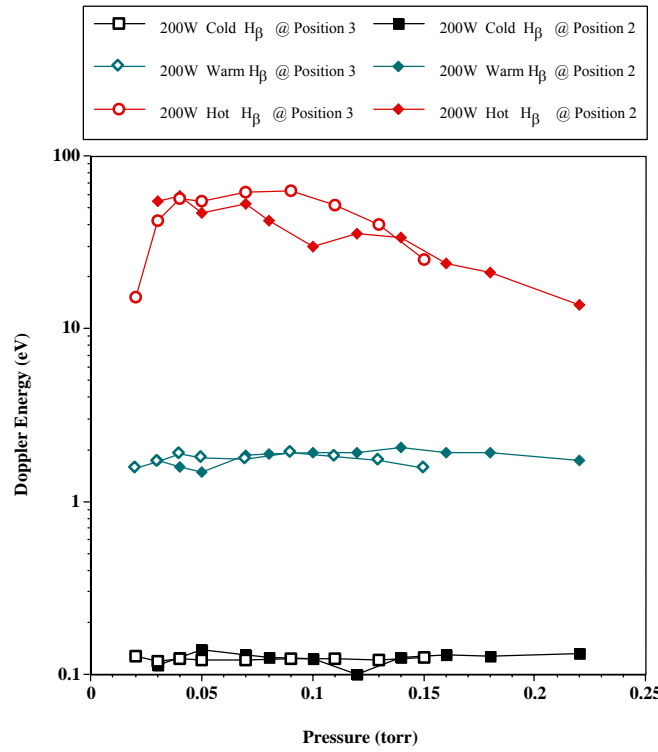
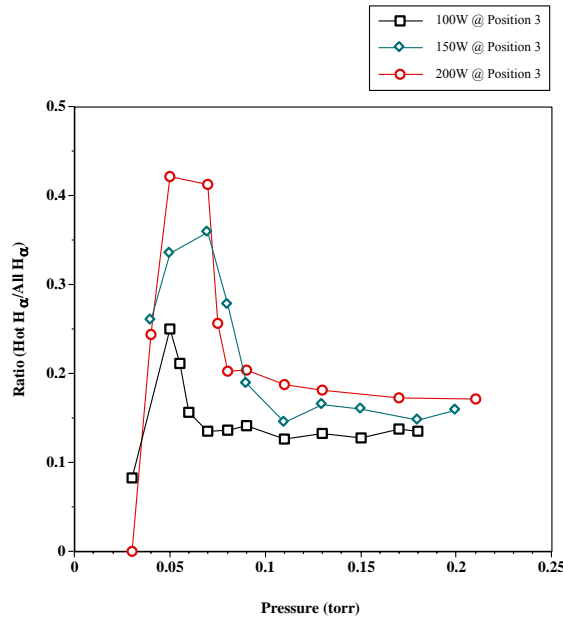
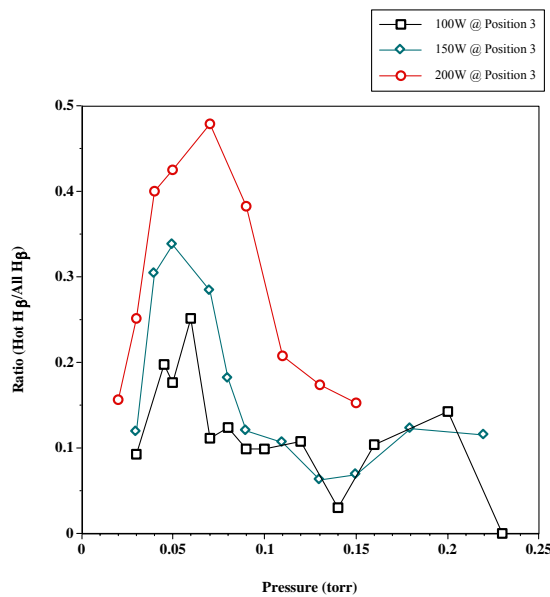


Figure 4. ‘Hot’ hydrogen between 10% and 45% of all atomic hydrogen. (a) and (b) At a position 15 cm from the electrode the fraction hot hydrogen varies as a function of pressure, and power to a lesser extent. Virtually identical trends are observed from the H α and H β data. (c) and (d) The trends in fraction hot hydrogen as a function of pressure and power are virtually identical between the plates and at 15 cm from the plates.

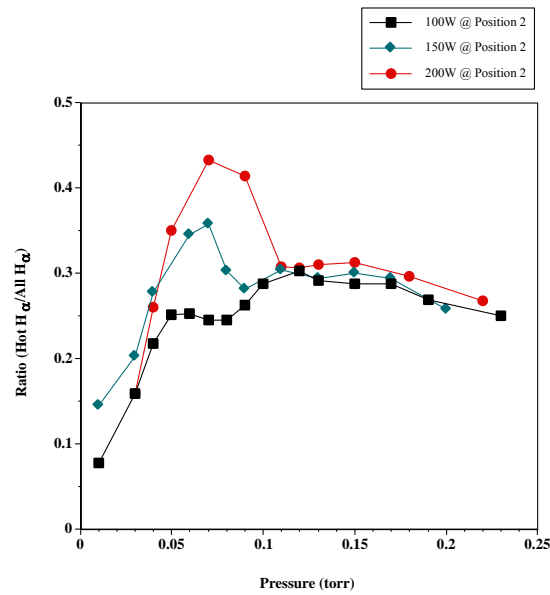
(a)



(b) Y axis: Ratio (Hot H α /All H β)



(c) Y axis: Ratio (Hot H α /All H β)



(d) Y axis: Ratio (Hot H α /All H β)

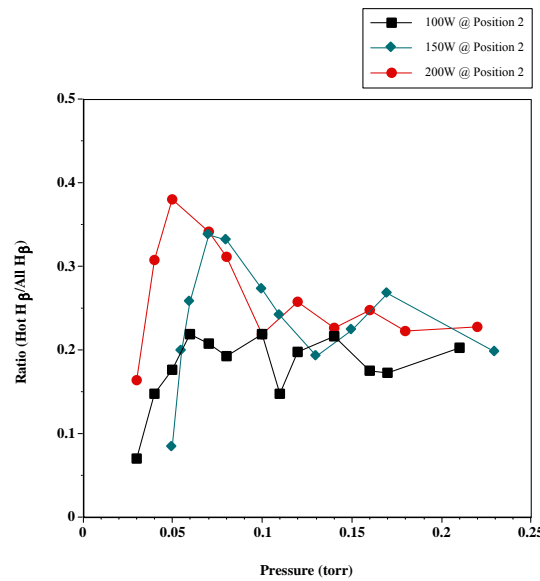
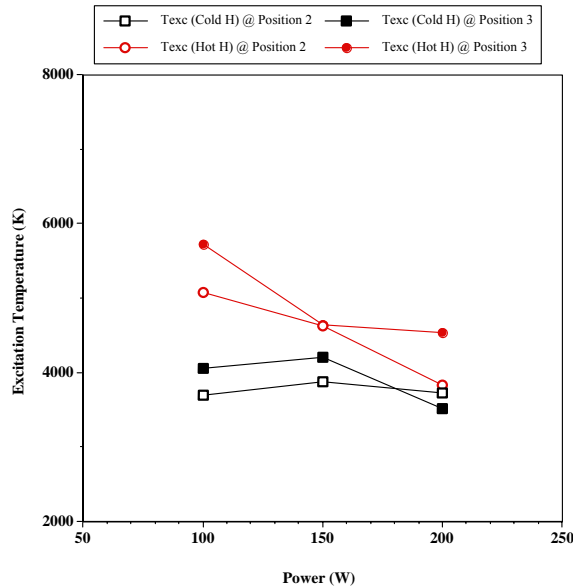


FIGURE 5. (a) Excitation energy (T_{exc}) determined as a function of power, position and hydrogen species used to determine peak intensity. (b) Boltzman plot showing the high fidelity of the data. Clearly computing excitation temperature on the ‘cold’ or ‘hot’ component of the line intensity makes only a small difference.

(a)



(b)

